

Magneto-Mechanical Bone Growth Stimulation by Actuation of Highly Porous Ferromagnetic Fibre Arrays

A.E. Markaki* and T.W. Clyne
Department of Materials Science & Metallurgy, University of Cambridge,
Pembroke Street, Cambridge CB2 3QZ, UK

ABSTRACT

This work relates to porous material made by bonding together fibres of a magnetic material. When subjected to a magnetic field, the array deforms, with individual fibres becoming magnetised along their length and then tending to line up locally with the direction of the field. An investigation is presented into the concept that this deformation could induce beneficial strains in bone tissue network in the early stages of growth as it grows into the porous fibre array. An analytical model has been developed, based on the deflection of individual fibre segments (between joints) experiencing bending moments as a result of the induced magnetic dipole. The model has been validated via measurements made on simple fibre assemblies and random fibre arrays. Work has also been done on the deformation characteristics of random fibre arrays with a matrix filling the inter-fibre space. This has the effect of reducing the fibre deflections. The extent of this reduction, and an estimate of the maximum strains induced in the space-filling material, can be obtained using a simple force balance approach. Predictions indicate that in-growing bone tissue, with a stiffness of around 0.01-0.1 GPa, could be strained to beneficial levels (~1 millistrain), using magnetic field strengths in current diagnostic use (~1 Tesla), provided the fibre segment aspect ratio is at least about 10. Such material has a low Young's modulus, but the overall stiffness of a prosthesis could be matched to that of cortical bone by using an integrated design involving a porous magneto-active layer bonded to a dense non-magnetic core.

Keywords: metal fibres, ferromagnetism, porosity, magneto-mechanical induction

1. INTRODUCTION

Implants must satisfy well-defined biological and mechanical requirements. The range of materials known to be bio-compatible, and in some cases bio-active, when in contact with bone tissue is now quite extensive. Certain structural metals, notably titanium alloys and some stainless steels, have good bio-compatibility and several surfaces treatments have been developed to encourage bone in-growth [1-6]. Mechanical requirements include sufficient strength to avoid plastic deformation, brittle fracture and fatigue crack propagation, preferably with a stiffness at least approximately matching that of bone, to minimise stress shielding. This latter effect, arises because prostheses are stiffer than surrounding bone, inhibiting it from being strained. (Most metals have a stiffness of about 100-200 GPa, whereas that of cortical bone is about 7-27 GPa). It is well known [7-9] that mechanical straining of bone is essential for healthy bone growth. The strain levels [7, 10] needed to promote beneficial bone growth effects are in the approximate range of 1-3 millistrain.

It has been repeatedly suggested [11-16] that making prostheses of porous metal might help to solve both the poor bonding and the stress shielding problems. Provided the pore size is suitable (~100-300 μm) [17] and the internal surfaces are bio-compatible or bio-active, bone in-growth can readily occur, leading to strong interfacial adhesion. Furthermore, stiffness reduction induced by porosity should reduce stress shielding. A possible problem [18, 19] with such highly porous metallic materials is that they are often mechanically weak, particularly in tension. However, certain types of porous metal, produced by bonding together metallic fibres [20], do exhibit promising strength and toughness levels.

2. EXPERIMENTAL PROCEDURES

2.1 Material and specimen production

Cylindrical specimens were made by brazing together an array of 446 (ferritic) stainless steel fibres, of diameter about 100 μm , melt extracted to lengths of about 4 mm (Fibretech Ltd). The porous specimens were created by spraying a small quantity (a few grams) of fibres with a (slow setting) aerosol glue and then sprinkling some braze powder (less than a gram) over them. The braze powder used, which is non-magnetic, has a composition (wt%) of

*am253@cam.ac.uk; Telephone: +44 (0)1223 334341; Fax: +44 (0)1223 334567; <http://www.msm.cam.ac.uk/mmc/>

Ni-14Cr-4Fe-2.8B-3.3Si-0.6C (Brazing & Soldering Automation Ltd). The fibres, with braze particles adhering to them, were packed into a 250 mm long quartz tube of 16 mm internal diameter. Brazing was carried out by holding at 1200°C for a few minutes.

Resultant specimens had porosity levels of about 75-90%. A typical fibre content and distribution is illustrated by the scanning electron micrograph shown in Fig.1. Some X-ray tomography has also been carried out to explore fibre orientations (Fig.2). While it's clear that the distributions produced were not fully isotropic, the tendency for fibres to lie in-plane was not predominant, with at least some fibre segments lying at relatively low angles to the axial direction (z).

Some fibre arrays were infiltrated in vacuum with a rubber (Evergreen™ 20, Smooth-On Inc.). The rubber was poured onto the sample and, on admitting air to the chamber, was forced into the interstitial spaces between fibres. To ensure complete penetration, several pumping-venting cycles were conducted. Curing then took place at room temperature.

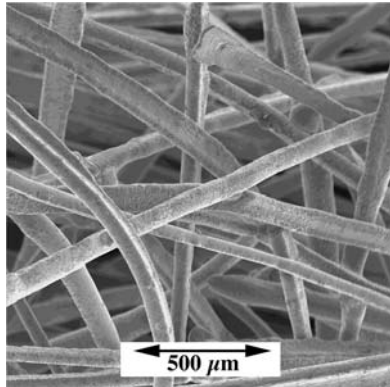


Fig.1: Scanning electron micrograph of a bonded fibre array material, made by brazing short ferritic stainless steel fibres.

Fig.2: X-ray tomographic image showing 3-D topology of a bonded fibre array. The axial direction (z) is also shown.

2.2 Stiffness measurements

Cylindrical specimens of the bonded fibre array material, about 15 mm long and about 14 mm in diameter, were loaded in axial compression on a servo-hydraulic testing apparatus equipped with a 1 kN load cell. The tests were conducted under displacement control, with a cross-head speed of 0.2 mm min⁻¹. The axial displacement was measured both via a LVDT and with a clip gauge extensometer. The axial stiffness was measured from the tangent of the unloading curves, within the elastic regime.

2.3 Magnetic measurements

Cylindrical specimens of the bonded fibre array material with or without surrounding matrix (rubber) were magnetically actuated by being placed between the pole pieces of a water-cooled DC electromagnet (Helmholtz coil), with the field direction parallel to the axis of the specimen. The uniform field region was about 50 mm in diameter and 30 mm in length. The maximum field strength was about 1 Tesla. Dimensional changes were measured using a scanning laser extensometer (Lasermike), with a resolution of about 1 μm.

3. MAGNETO-MECHANICAL ACTUATION

3.1 Magnetic deflection model

An analytical magneto-mechanical model has been developed [21] which can be used to estimate the distortions induced in a free-standing porous specimen by application of a magnetic field. The model is based on the deflection of individual fibre segments (between joints) experiencing bending moments as a result of the induced magnetic dipole. These segments act like pairs of cantilever encasté beams, joined at segment mid-points. The geometry of such deflections is illustrated in Fig.3. Δz and Δr are respectively the relative deflections of the fibre mid-points parallel and normal to the applied field B . The model has been validated by constructing simple fibre assemblies [21].

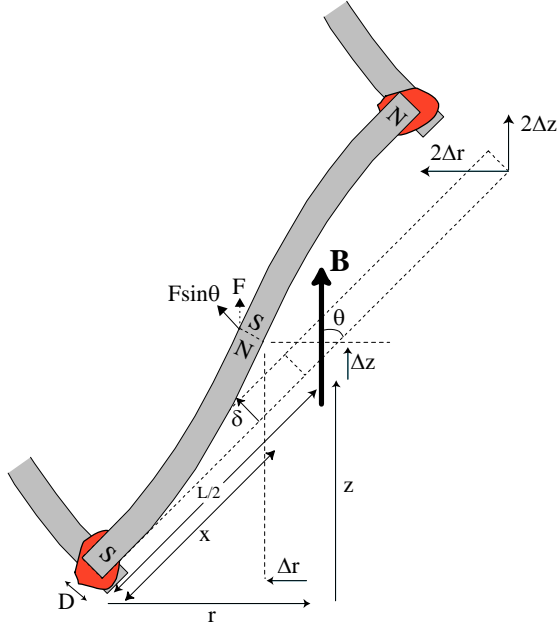


Fig.3: Schematic representation of the deflection of a fibre segment within a fibre array, under the influence of an applied magnetic field, B . δ is the deflection at a distance x along an end-loaded cantilever beam and θ is the angle between the fibre axis and the magnetic field axis.

3.2 Deformation of a random fibre array

Prediction of the deformation characteristics of a three-dimensional array of bonded fibres is complex, particularly if they are not in a regular arrangement. For a random fibre orientation distribution, the deflection of a fibre segment will be constrained by neighbouring segments. However, if it is assumed that, averaged over the volume, constraint effects will cancel out, then the overall deformation can be predicted by summing the contributions from individual segments, taken in isolation. The net axial extension ($\Delta Z/Z$) and the net transverse contraction ($\Delta R/R$) are predicted [21] to conform to Eqns. (1) and (2) respectively.

$$\frac{\Delta Z}{Z} = \left(\frac{16M_s B}{9E_f} \right) \left(\frac{L}{D} \right)^2 \quad (1)$$

$$\frac{\Delta R}{R} = \left(\frac{-16M_s B}{9\pi E_f} \right) \left(\frac{L}{D} \right)^2 \quad (2)$$

where B is the applied field, M_s is the saturation magnetisation, E_f is the fibre modulus and L , D are the fibre length and diameter respectively.

The resultant deformation of the fibre array generates a shape change, as illustrated in Fig.4. Predicted shape changes obtained using Eqns. (1) and (2) are presented in Fig.5, as a function of fibre segment aspect ratio, L/D . Also included on this plot is measured axial extension for a free-standing fibre array. (The fibre segment aspect ratios for the bonded fibre arrays were estimated from SEM micrographs, such as the one shown in Fig.1.) It can be seen that the measured deflections are larger than those predicted by the model. While close agreement with experiment is not really expected here, since in reality the deformation behaviour of a fibre network is expected to be complex, it is important to note that magnetically-induced shape changes can be substantial, particularly for large L/D .

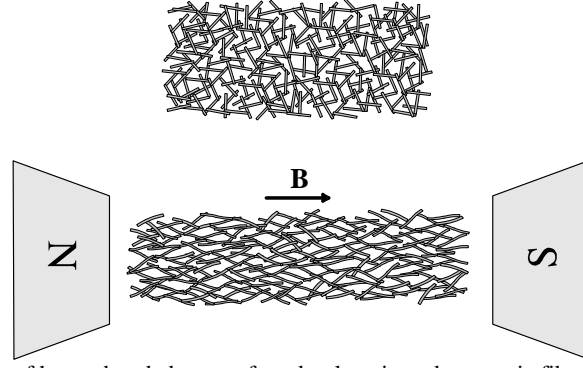


Fig.4: Schematic representation of how a bonded array of randomly-oriented magnetic fibres will deform in a magnetic field.

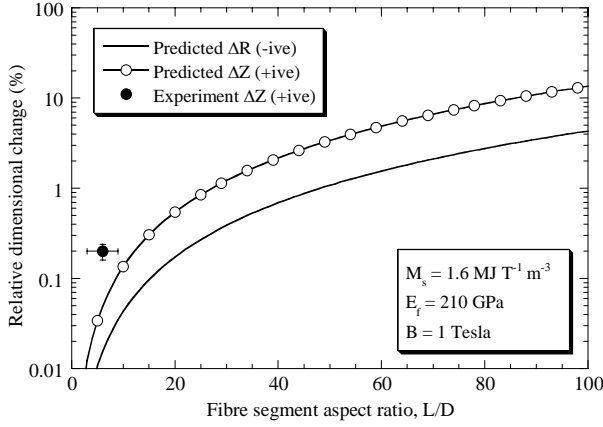


Fig.5: Predicted dependence on fibre segment aspect ratio of shape changes induced in a 3-D random fibre array, on applying a magnetic field of 1 Tesla. Experimental data for fibre arrays with $L/D \sim 6$ are also shown.

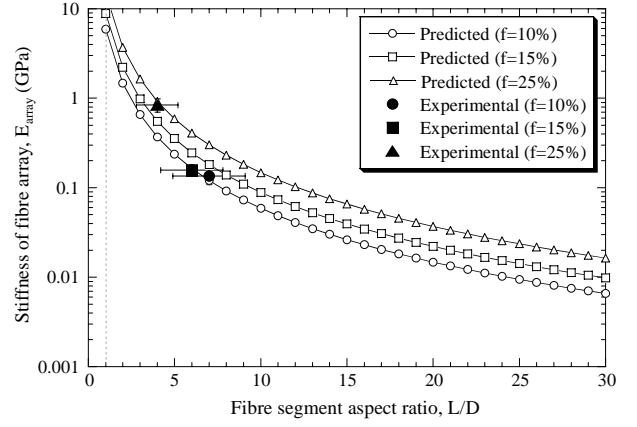


Fig.6: Predicted dependence on fibre segment aspect ratio and fibre volume fraction of the stiffness of a 3-D random fibre array. Experimental data for fibre arrays with different L/D and f values are also shown

The stiffness of the array, E_{array} , can also be predicted, using a similar approach [21]. The analysis leads to Eqn.(3). This depends on fibre volume fraction, f , as well as segment aspect ratio, L/D . Comparisons with experimental data are presented in Fig.6. While predictions are in good agreement with the measured values, it can be seen that only with a low L/D ($< \sim 5$), the stiffness of the array could be matched to that of cortical bone (~ 10 GPa).

$$E_{array} = \frac{9E_f f}{32 \left(\frac{L}{D}\right)^2} \quad (3)$$

3.3 Straining of material within a fibre array

The model can be extended to predict the deformation of a fibre array when the space between the fibres is filled with a material (ie an environment) of specified stiffness, E_c . This has the effect of reducing the fibre deflections (Fig.7). An estimate of the maximum strains induced in the space-filling material can be obtained using a simple force balance approach [21]. The analysis leads to Eqn.(4). Strains are calculated between a pair of fibres, symmetrically oriented on opposite sides of the magnetic field axis, as shown in Fig.7(b).

$$\varepsilon_{max} \approx \frac{12\pi M_s B \sin \theta \left(\frac{L}{D}\right)^2}{\left(9\pi E_f \tan \theta + 28E_c \left(\frac{L}{D}\right)^3\right)} \quad (4)$$

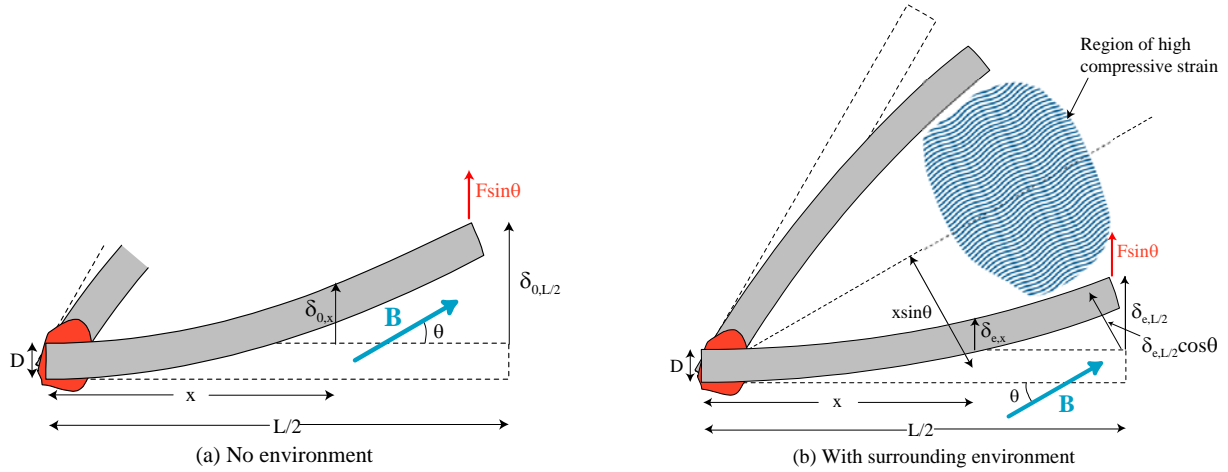


Fig.7: Schematic representation of the elastic deformation of a bonded pair of fibres, with and without a surrounding environment of finite stiffness.

Predictions are shown in Fig.8, for several matrix stiffness levels. It can be seen that strain levels expected to be physiologically beneficial (~ 1 millistrain) could be generated, particularly with relatively high segment aspect ratios. For example, with a fibre segment aspect ratio of 10, it would be possible, by applying a field of 1 T, to induce strains of around 1 millistrain in surrounding bone (which typically has a stiffness of the order of 0.01-0.1 GPa). It is clear that these strains are decreasing as the constraint imposed by the surrounding material increases. The effect of the presence of the environment on the induced strain can also be predicted [22]. This is found to depend on the segment aspect ratio, L/D , and the matrix/fibre stiffness ratio, E_e/E_f . Predictions are presented in Fig.9 and are at least broadly consistent with experimental results obtained from rubber-impregnated arrays.

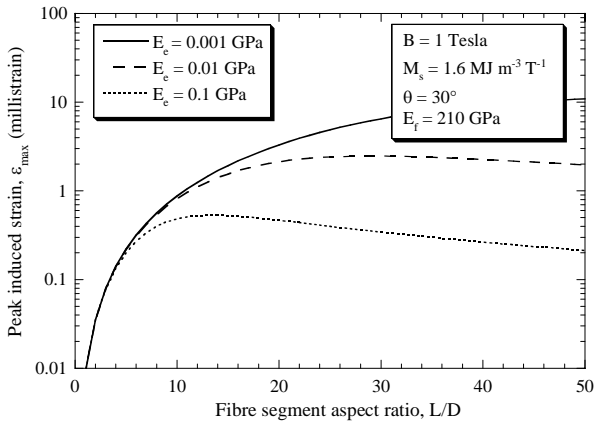


Fig.8: Predicted dependence on fibre aspect ratio of the peak strain generated within a surrounding environment on applying a magnetic field of 1 Tesla to a porous material made of bonded fibres.

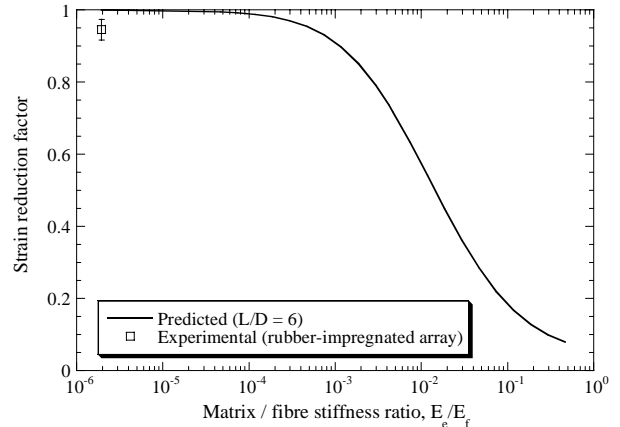


Fig.9: Predicted dependence on matrix / fibre stiffness ratio, E_e/E_f , of the strain reduction induced in a bonded-fibre porous material by the presence of a matrix. Also shown are experimental data for rubber-impregnated fibre arrays with $L/D \sim 6$.

4. INTEGRATED PROSTHESIS DESIGN

Model predictions (Figs. 6 and 8) indicate that it is difficult to design a single material with (a) sufficiently high fibre segment aspect ratio to confer the potential for magneto-mechanical induction of therapeutically beneficial strains and (b) low enough aspect ratio to be sufficiently stiff to provide a good match with that of bone. However, an integrated design involving a porous magneto-active layer bonded to a dense non-magnetic core would allow such an effect to be exploited - see Fig.10. The porous layer, into which bone growth would occur and within which magneto-mechanical stimulation could be induced, would need to be relatively thick, since the regions immediately adjacent to the core would be constrained from deforming under the influence of a magnetic field. By varying the relative sectional areas of the two constituents, it should be possible to tailor the overall stiffness of the device to match that of bone.

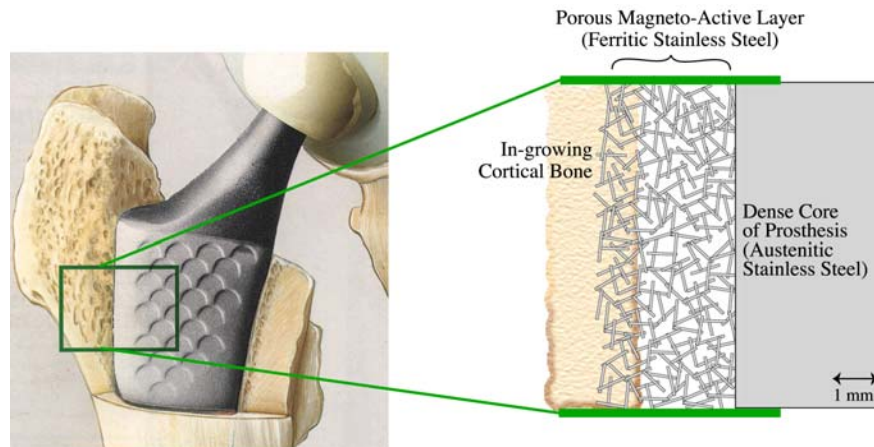


Fig.10: Schematic depiction of a magneto-active porous layer on a dense prosthesis.

CONCLUSIONS

This work relates to material made up of ferromagnetic fibres, which are strongly bonded together at cross-over points. When a magnetic field is applied, a fibrous array of this type deforms elastically, as a result of the tendency for such fibres to align with the field. In-growing bone tissue filling the inter-fibre space would be mechanically strained during such deformation. The following conclusions can be drawn from this work.

- A simple analytical model, based on the deflection of a single ferromagnetic fibre in a magnetic field, has been used to predict the shape changes induced in a fibre array. The model indicates that the fibre segment aspect ratio, L/D , represents an important design parameter. The resulting predictions are at least broadly consistent with limited experimental data, obtained using free-standing random fibre arrays.
- An expression has been derived for the Young's modulus of such material, relative to that of the fibres, as a function of the fibre segment aspect ratio, L/D , and the fibre volume fraction, f . It can be seen that only with a low L/D ($< \sim 5$), the stiffness of the array could be matched to that of cortical bone (~ 10 GPa). Good agreement has been observed with measured values for fibre arrays with different L/D and f values.
- A model has also been used for prediction of the deformation of a fibre array when the inter-fibre space is filled with a (compliant) matrix. This results in reduction of the induced strains and is dependent on the matrix/fibre stiffness ratio, E_c/E_f , and the fibre segment aspect ratio, L/D . Experimental data from fibre arrays infiltrated with rubber are in reasonable agreement with predictions.
- Model predictions indicate that, using magnetic fields already employed for diagnostic properties (~ 1 Tesla), it should be possible to induce physiologically beneficial strains ($> \sim 1$ millistrain) in in-growing bone, provided the fibre segment aspect ratio is at least about 10. However, such material has a low stiffness. The stiffness of the prosthesis could be matched to that of cortical bone by using an integrated design involving a porous magneto-active layer bonded to a dense non-magnetic core.

ACKNOWLEDGEMENTS

Support comes from the Cambridge-MIT Institute (CMI), within a project on the development of novel sheets and materials incorporating metallic fibres, and from the EPSRC (Gordon Laboratory Platform Grant). The authors are grateful to Dr. Eric Maire (GEMPPM, INSA de Lyon) for carrying out the X-ray tomography.

REFERENCES

1. K. De Groot, R. Geesink, C.P.A.T. Klein, and P. Serekian, Plasma Sprayed Coatings of Hydroxyapatite. *J. Biomed. Mater. Res.*, 1987. 21: p. 1375-1381.
2. W.R. Lacefield, Hydroxyapatite Coating. *N. Y. Acad. Sci.*, 1988. 523: p. 72-80.
3. M. Shirkhazadeh, Bioactive Calcium Phosphate Coatings prepared by Electrodeposition. *J. Mater. Sci. Letters*, 1991. 10: p. 1415-1421.
4. P. Ducheyne, W. Van Raemdonck, J.C. Heughbaert, and M. Heughbaert, Structural Analysis of Hydroxyapatite Coatings on Titanium. *Biomaterials*, 1986. 7: p. 97-103.

5. S. Nishiguchi, H. Kato, H. Fujita, H.M. Kim, F. Miyaji, T. Kokubo, and T. Nakamura, Enhancement of Bone Bonding Strengths of Titanium Alloy Implants by Alkali and Heat Treatments. *J. Biomed. Mater. Res. (Appl. Biomater.)*, 1999. 48: p. 689-696.
6. H.M. Kim, H. Takadama, T. Kokubo, S. Nishiguchi, and T. Nakamura, Formation of a Bioactive Graded Surface Structure on Ti-15Mo-5Zr-3Al Alloy by Chemical Treatment. *Biomaterials*, 2000. 21: p. 353-358.
7. H.M. Frost, Bone "Mass" and the "Mechanostat": A Proposal. *Anatomical Record*, 1987. 219(1): p. 1-9.
8. J.R. Mosley, Osteoporosis and Bone Functional Adaptation: Mechanobiological Regulation of Bone Architecture in Growing and Adult Bone, a Review. *J. Rehab. Res. & Develop.*, 2000. 37: p. 189-199.
9. O. Akhouayri, M.H. Lafage-Proust, A. Rattner, N. Laroche, A. Caillot-Augusseau, C. Alexandre, and L. Vico, Effects of Static or Dynamic Mechanical Stresses on Osteoblast Phenotype Expression in Three-Dimensional Contractile Collagen Gels. *J. Cellular Biochemistry*, 2000. 76: p. 217-230.
10. C.T. Rubin and L.E. Lanyon, Regulation of Bone Mass by Mechanical Strain Magnitude. *Calcif. Tissue Int.*, 1985. 37: p. 411-417.
11. Y.S. Chang, M. Oka, M. Kobayashi, H.O. Gu, Z.L. Li, T. Nakamura, and Y. Ikada, Significance of Interstitial Bone Ingrowth under Load-bearing Conditions: A Comparison between Solid and Porous Implant Materials. *Biomaterials*, 1996. 17(11): p. 1141-1148.
12. M. Oka, Y.S. Chang, T. Nakamura, K. Ushio, J. Toguchida, and H.O. Gu, Synthetic Osteochondral Replacement of the Femoral Articular Surface. *J. Bone & Joint Surgery (UK)*, 1997. 79(6): p. 1003-1007.
13. D.W. Hutmacher, Scaffolds in Tissue Engineering Bone and Cartilage. *Biomaterials*, 2000. 21: p. 2529-2543.
14. J.W. Vehof, M.T. Haus, A.E. de Ruijter, P.H. Spauwen, and J.A. Jansen, Bone Formation in Transforming Growth Factor Beta-I-Loaded Titanium Fiber Mesh Implants. *Clinical Oral Implants Research*, 2002. 13(1): p. 94-102.
15. S.B. Kang, K.S. Yoon, J.S. Kim, T.H. Nam, and V.E. Gjunter, In vivo Result of Porous TiNi Shape Memory Alloy: Bone Response and Growth. *Materials Transactions, JIM*, 2002. 43: p. 1045-1048.
16. T. Livingston, P. Ducheyne, and J. Garino, In vivo Evaluation of a Bioactive Scaffold for Bone Tissue Engineering. *J. Biomed. Mater. Res.*, 2002. 62: p. 1-13.
17. J.D. Bobyn, R.M. Pilliar, H.U. Cameron, and G.C. Weatherly, The Optimum Pore Size for the Fixation of Porous-Surfaced Metal Implants by the Ingrowth of Bone. *Clin. Orth. and related research*, 1980(150): p. 263-270.
18. L.J. Gibson, Mechanical Behaviour of Metallic Foams. *Ann. Rev. Mater. Sci.*, 2000. 30: p. 191-227.
19. A.E. Markaki and T.W. Clyne, The Effect of Cell Wall Microstructure on the Deformation and Fracture of Aluminium-Based Foams. *Acta Mater.*, 2001. 49(9): p. 1677-1686.
20. P. Ducheyne, E. Aernoudt, and P. De Meester, The Mechanical Behaviour of Porous Austenitic Stainless Steel Fibre Structures. *J. Mater. Sci.*, 1978. 13: p. 2650-2658.
21. A.E. Markaki and T.W. Clyne, Magneto-Mechanical Stimulation of Bone Growth in a Bonded Array of Ferromagnetic Fibres. *Biomaterials*, 2004. 25(19): p. 4805-4815.
22. A.E. Markaki and T.W. Clyne, Magneto-Mechanical Actuation of Bonded Ferromagnetic Fibre Arrays, in *Acta Mater.* 2005. in press.